ISSN 1660-6795
www.nano-ntp.com

Novel Green Synthesis of Gold Nanoparticles from *Scolopia crenata* Stem Bark Extract: Evaluation of Anti-Inflammatory, Wound Healing, and Anticancer Activities.

Mahanthesh Kumar G.T,[1] Ramesh C. K,[1*] V. Krishna,[2] Sowmyashree A S,[3] Abdul Shafiulla,[1] Pallavi M.[1]

[1]Phytomedicine Laboratory, Department of Postgraduate Studies and Research in Biotechnology, Sahyadri Science College, Kuvempu University, Shivamogga Karnataka 577203

[2]Department of Postgraduate Studies and Research in Biotechnology and Bioinformatics, Jnana Sahyadri Shankaraghatta, Shivamogga Karnataka 577451

[3]Department of Chemistry, Nitte Meenakshi institute of technology, Bangalore- Indian. 560064

Corresponding author*

Dr. Ramesh C. K. E-mail: ckramck@gmail.com

Professor, Phytomedicine Laboratory, Department of Postgraduate Studies and Research in Biotechnology, Sahyadri Science College, Kuvempu University, Shivamogga Karnataka 577203

Abstract

Gold nanoparticles (AuNPs) have gained significant attention in biomedical applications due to their unique properties. This study explores an eco-friendly synthesis method for AuNPs using the stem bark extract of Scolopia crenata, an endemic medicinal plant from India, and investigates their pharmacological potential. AuNPs were synthesized using *S. crenata* stem bark extract and characterized using UV-visible spectroscopy, FTIR, XRD, SEM, zeta potential, and particle size analyses. The nanoparticles were evaluated for anti-inflammatory activity through protein denaturation assays, wound healing potential via scratch assays on fibroblast cells, and anticancer efficacy against MDA-MB-231 and A549 cell lines using MTT assays. The synthesized AuNPs exhibited stability, crystalline structure, and an average size range of 71.9-100 nm. In vitro studies demonstrated significant anti-inflammatory effects through inhibition of inflammatory mediators, enhanced wound healing activity by promoting cell migration and proliferation, and notable cytotoxic effects against human cancer cell lines. This study presents a novel, eco-friendly approach for synthesizing AuNPs using *S. crenata* stem bark extract. The resulting nanoparticles showed promising anti-inflammatory, wound-healing, and anticancer properties, highlighting their potential for therapeutic applications and emphasizing the role of endemic medicinal plants in advancing nanotechnology and biomedical science.

Keywords: Nanotechnology, gold nanoparticles, anti-inflammatory, scratch assay, anticancer.

1. INTRODUCTION

Nanotechnology has significantly advanced the fields of science and medicine by offering novel solutions to longstanding challenges [1]. Among various types of nanoparticles, gold nanoparticles (AuNPs) have garnered substantial attention owing to their distinctive properties[2], including facile synthesis, stability, and biocompatibility, which render them suitable for diverse biomedical applications [3]. Traditional methods for synthesizing AuNPs often involve hazardous chemicals and high energy consumption, raising environmental and safety concerns [4]. Green synthesis of AuNPs using plant extracts is a sustainable and eco-friendly alternative that adheres to the principles of green chemistry [5]. This method utilizes natural reducing and stabilizing agents present in plant extracts to effectively reduce gold ions (Au^3+) to AuNPs under mild conditions [6]. This approach not only minimizes the use of toxic chemicals but also enhances the biocompatibility of nanoparticles, making them more suitable for in vitro applications [7, 8]. Among the various plant sources investigated for green synthesis, *Scolopia crenata*(W&A) Clos, a medicinal plant endemic to India, is noteworthy because of its rich phytochemical profile and traditional medicinal uses. Scolopia crenata, belonging to the family Flacourtiaceae [9], is renowned for its therapeutic properties, including anti-inflammatory, antioxidant, and wound-healing activities. Phytochemicals in the stem bark of *Scolopia crenata*, such as flavonoids, tannins, and phenolic compounds, are known to possess potent biological activities, making them ideal candidates for green synthesis of AuNPs. The interaction between these bioactive compounds and Au ions leads to the formation of AuNPs with unique physicochemical properties and enhanced pharmacological potential.

The primary objective of this study was to synthesize AuNPs using the aqueous stem bark extract of *S. crenata*, characterize the synthesized nanoparticles, and evaluate their *in vitro* pharmacological activities, including antioxidant, anti-inflammatory, wound-healing, and anticancer properties. The characterization of AuNPs is essential for confirming their formation and understanding their structural and functional attributes. Techniques such as UV-visible spectroscopy, Fourier-transform infrared spectroscopy (FTIR), X-ray diffraction (XRD), scanning electron microscopy (SEM), zeta potential analysis, and particle size analysis (PSA) are employed to determine the size, shape, crystallinity, and surface chemistry of nanoparticles [10]. Anti-inflammatory activity was assessed using protein denaturation assays, a standard method for evaluating the inhibition of inflammatory mediators [11]. Inflammation, a common pathological condition associated with numerous diseases, requires effective anti-inflammatory agents for therapeutic intervention [12]. Wound healing, a complex process involving multiple cellular and molecular events, was evaluated using scratch assays in fibroblast [13]. This in vitro assay mimics the wound healing process and measures the percentage of cell migration and proliferation, which are crucial for tissue repair and regeneration [14]. The ability of AuNPs to enhance these processes suggests their potential application in wound-healing therapies. The anticancer activity of the synthesized AuNPs was tested against human cancer cell lines, including MDA-MB-231 (breast cancer) and A549 (lung cancer), using the MTT assay [15]. The MTT assay was used to measure cell viability and cytotoxicity. These results provide insights into the potential of AuNPs as anticancer agents, highlighting their ability to selectively target and eradicate cancer cells while sparing normal cells [16]. This study integrates green synthesis with the pharmacological evaluation of AuNPs derived from *Scolopia crenata* stem bark extract, offering a novel approach for developing multifunctional

therapeutic agents. This study contributes to the growing body of knowledge on green nanotechnology and underscores the potential of utilizing endemic medicinal plants in biomedical applications. This eco-friendly synthesis method aligns with sustainable development goals, reducing the environmental impact associated with conventional nanoparticle synthesis.

2. METHODS AND MATERIALS

2.1. Collection of Plant Material and Preparation of Extract

The stem bark of *Scolopia crenata*(W&A) Clos was collected from Gini-Gini Honnavalli Post, Sringeri Rural, Balehonnuru Range, near the Rainforest Office, Sringeri Taluk, Chikkamagaluru District, Karnataka, India-577112. The plant was identified by the Adithya Rao G S, Deputy Range Forest Officer, Government of Karnataka. A herbarium specimen (SSC/DB/2022/0049) was deposited in the Department of Botany, Sahyadri Science College. The collected stem bark was thoroughly washed with distilled water to eliminate any dirt and impurities and then shade-dried for two weeks. Once dried, the stem bark was ground to a fine powder using a mechanical grinder. To prepare the extract, 10 g of the stem bark powder was mixed with 100 mL of distilled water. The mixture was then filtered through Whatman No. 1 filter paper and the filtrate was collected in a separate flask.

2.2. Synthesis of *S. crenata* stem bark aqueous extract gold nanoparticles

Aqueous plant extract (1 mL) was added to 10 mL of 1 mM gold chloride solution. The reaction mixture was then incubated in the dark at ambient temperature to mitigate unwanted photochemical reactions [17]. A colorimetric shift was observed in the reaction mixture over time; the initially colorless solution gradually transitioned to blue and ultimately to a dark red color, signifying the synthesis of the nanoparticles. After the reaction, the mixture was centrifuged at 10,000 rpm for 10 min. This centrifugation process was repeated to eliminate any residual plant extract, after which the metal nanoparticles were redispersed in double-distilled water, dried, and collected in powder form [18].

2.3. Structural characterization of biosynthesized gold nanoparticles

A series of analytical techniques was employed to characterize the physicochemical properties of the synthesized gold nanoparticles (AuNPs), a series of analytical techniques were employed. Ultraviolet-visible (UV–vis) absorption spectra were acquired using a Cary 100 UV–vis spectrometer across the wavelength range of 200–800 nm with quartz cuvettes[19]. Fourier-transform infrared spectroscopy (FTIR) was performed using a Thermo Nicolet 6700 spectrometer to detect functional groups within the 200–4000 cm^{-1} range[20]. The crystallinity of the AuNPs was determined by X-ray diffraction (XRD) using a Shimadzu XRD-7000 instrument [21]. The surface morphology and particle size were analyzed using scanning electron microscopy (SEM) with a JEOL JEM 2100 model operating at 90 kV, including high-resolution SEM imaging[22]. Additionally, the surface charge of the synthesized AuNPs was assessed using a zeta potential analyzer (HORIBA Nanoparticle Analyzer SZ100) [23].

2.4. Evaluation of *in vitro* anti-inflammatory activity

The anti-inflammatory effects of the aqueous stem bark extract of *Scolopia crenata* and its gold nanoparticles (AuNPs) were assessed using a protein denaturation assay, with modifications as outlined in references. Aspirin served as the standard pharmaceutical comparator. The procedure entailed the preparation of a reaction mixture by combining 2 mL of a commercially available AuNP solution at a concentration of 100 µg/mL with an equivalent volume of a

standard aspirin solution at 100 µg/mL. To this mixture, 0.1 mL of phosphate-buffered saline (pH 6.4) was added to this mixture, followed by 2 mL of fresh hen egg albumin (1 mM). The mixture was incubated at 27°C ±1°C for 15 min, after which protein denaturation was induced by heating the reaction mixture to 70°C for 10 min in a water bath. Upon cooling, absorbance was measured at 660 nm using double-distilled water as a blank [24]. The experiment was conducted in triplicate and the percentage inhibition of protein denaturation was calculated using the following formula:

$$\% \text{ Protein denaturation activity} = [(Ac - As)/Ac] \times 100 \text{----------(1)}$$

Where Ac is the absorbance of the control and As is the absorbance in the presence of the extract or standard sample.

2.5. Evaluation of *in vitro* wound healing activity

L929 fibroblast cells were trypsinized and transferred to a 5 mL centrifuge tube. After centrifugation at 300 g, a cell pellet was obtained. The cell concentration was adjusted using DMEM. In each well of a 12-well plate, 1 mL of DMEM containing 100 µL of the cell suspension was added. The plate was incubated at 37°C in a 5% CO_2 atmosphere for 24 h to achieve approximately 100% confluency as a monolayer. Without changing the medium, a scratch was made gently and slowly across the center of the monolayer using a new 200 µL pipette tip, ensuring that the long axis of the tip was perpendicular to the bottom of the well during scratching. The gap distance was determined based on the outer diameter of the pipette tip, which was adjusted using different tip sizes. Scratching was performed along a straight line in one direction. After scratching, the wells were gently washed twice with medium to remove detached cells, followed by two washes with 1× PBS. PBS was aspirated, and the wells were replenished with fresh medium. Test drug concentrations from the stock solution were added to the respective wells, along with 1 mL of fresh medium. Photographs of the scratched monolayer were taken at various time points (0, 6, 12, and 24 h) with subsequent incubation of the plate at 37°C and 5% CO_2 during these intervals[25, 26]. The gap distance was quantitatively assessed using MagVision Software with measurement calibration at 4× magnification. The migration rate was calculated using the following equation:

$$\% \text{ of Wound Closure} = \text{Initial wound diameter-Final diameter} \div \text{Initial diameter X } 100 \text{-----(2)}$$

2.6. Evaluation of *in vitro* anticancer activity of gold nanoparticles using MTT assay

To evaluate the potential biomedical application of this material, its cytotoxicity must be assessed. The in vitro cell viability assay is an effective method to obtain reliable data on the cytocompatibility of newly developed nanomaterials. The cytotoxic effects of *Scolopia crenata* and its synthesized gold nanoparticles (AuNPs) were analyzed using noncancerous fibroblast cells (L929), while their anticancer efficacy was evaluated in lung cancer (A549) and breast cancer (MDA-MB-231) cell lines using the standard MTT assay. All cell lines were acquired from the National Center for Cell Science (NCCS), Pune, India. The IC50 values, representing the concentration at which cell growth was inhibited by 50%, were determined by constructing dose-response curves for each cell line [27, 28]. The percentage of growth inhibition was calculated using the following formula:

$$\text{Inhibition Percentage} = \text{OD of Test sample} \div \text{OD of control} \times 100 \text{-----(3)}$$

where the OD of the test sample refers to the absorbance of the sample with the test material and the OD of the control represents the absorbance of the control reaction (which includes all reagents except the test material). The yellow tetrazolium compound MTT (3-(4,5-

dimethylthiazolyl-2)-2,5-diphenyltetrazolium bromide) is reduced by metabolically active cells through the action of dehydrogenase enzymes, producing reducing equivalents such as NADH and NADPH.

3. STATISTICAL ANALYSIS

The biological activity data were analyzed using SPSS version 20.0 with analysis of variance (ANOVA). The significance level was set at ($p>0.05$), and Duncan's Multiple Range Test (DMRT) was used to determine significant differences between the means. Data are presented as mean ± standard error (SE).

4. RESULT

4.1. Synthesis and characterization of newly synthesized AuNPs using an aqueous extract of *S. crenata* stem bark extract

This study focused on the synthesis of gold nanoparticles (AuNPs) using an eco-friendly plant-mediated approach. The formation of AuNPs was visually confirmed by a color change from brown to dark red after 2 h of incubation, indicating completion of the reaction (Figure 1). This color transition typically reflects changes in the oxidation state of the metal, with Au^{+} reduced to Au^{0} by unidentified molecules in S. crenata. The observed color change is attributed to the excitation of the surface plasmon resonance in the AuNPs.

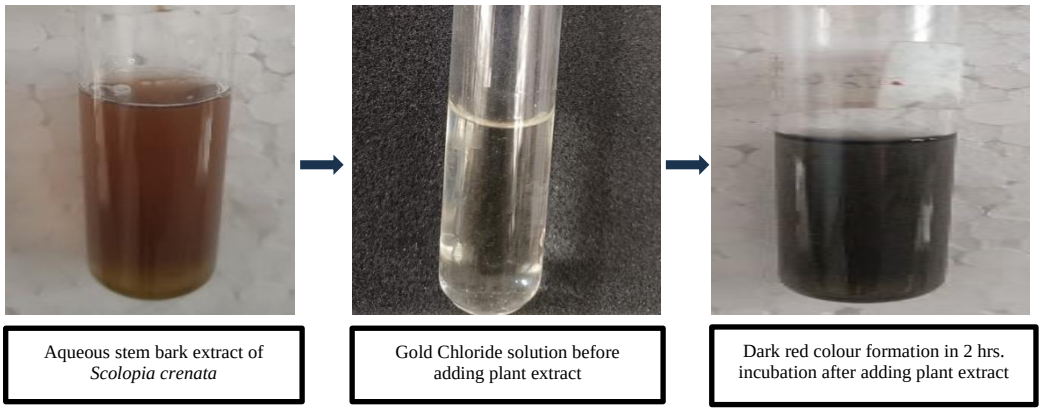

Figure 1. Formation of AuNPs using aqueous stem bark extract of *S. crenata* with 10 mM gold chloride solution.

4.2. UV-Visible Spectroscopy

The formation of gold nanoparticles was initially confirmed by observing color changes, which were further validated using a UV-visible spectrophotometer, a highly effective technique for analyzing metal nanoparticles. The UV-visible spectra (Figure-2) displayed a distinct plasmon resonance peak at 550 nm for the AuNPs synthesized using the aqueous stem bark extract of *S. crenata*. The presence of this strong and broad plasmon peak is a well-documented feature of AuNPs, typically indicating particle sizes ranging from 1 nm to 100 nm.

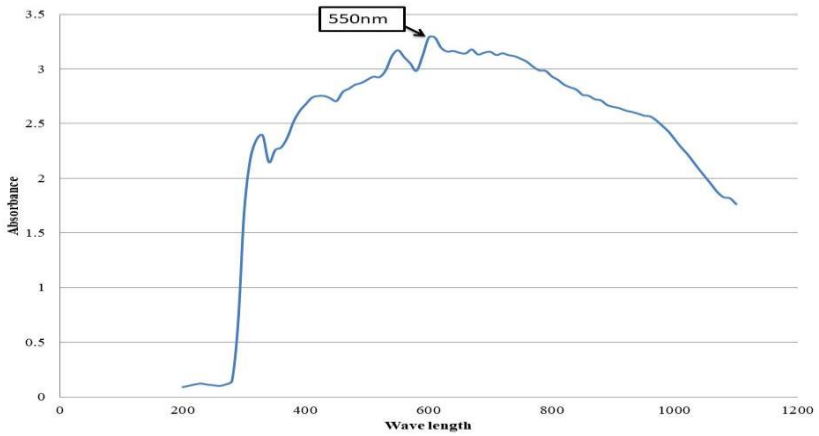

Figure 2. UV-VIS spectral analysis of AuNPs synthesized from aqueous stem bark extract of *S. crenata*

4.3. Fourier transform infrared spectroscopy (FTIR) studies

The FTIR spectrum of the AuNPs synthesized using the aqueous stem bark extract of *Scolopia crenata* was analyzed to identify the functional groups involved in the reduction of Au + to Au^0 nanoparticles. The infrared spectra of both the plant extract and AuNPs revealed the presence of various functional groups, including alkanes, nitro compounds, alkyls, esters, carboxylic acids, alkynes, sulfonamides, allenes, isothiocyanates, ketones, thiocyanates, ketenes, nitriles, carbon dioxide, and carboxylic acids (as illustrated in Figure-3). The FTIR analysis of the AuNPs identified significant peaks at 2560 cm^{-1}, 2500 cm^{-1}, 2352 cm^{-1}, 2224 cm^{-1}, 2184 cm^{-1}, 2162 cm^{-1}, 2115 cm^{-1}, 2051 cm^{-1}, 1998 cm^{-1}, 1951 cm^{-1}, 1909 cm^{-1}, 1635 cm^{-1}, 1338 cm^{-1}, and 1175 cm^{-1}. These functional groups are likely essential in the synthesis of nanoparticles from plant material, playing roles in capping, stabilizing, and reducing the particles, as summarized in (Table 1).

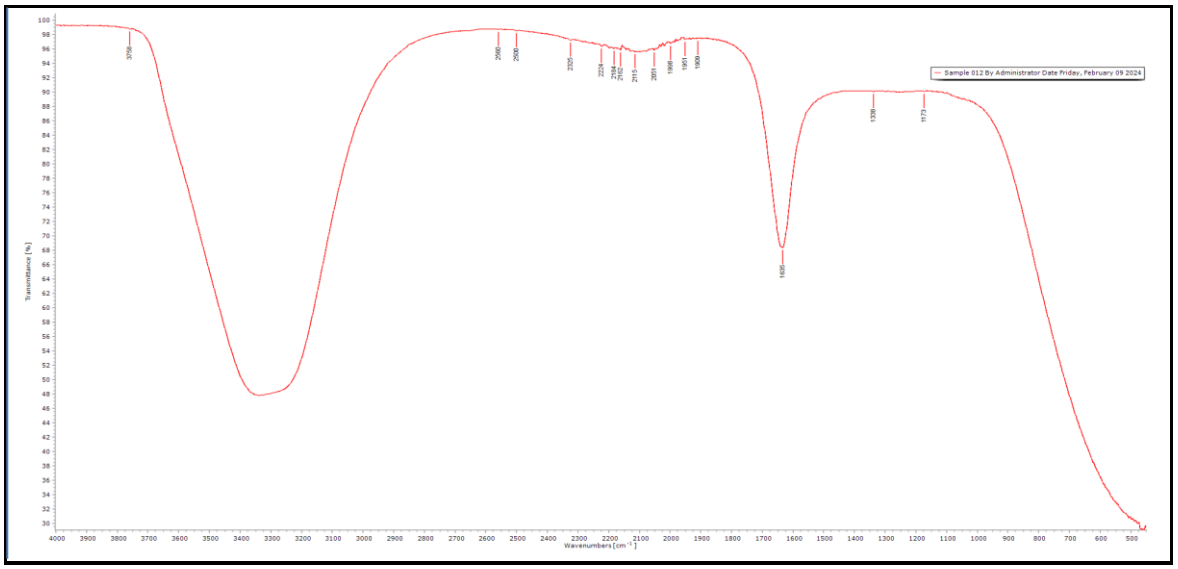

Figure-3: FTIR spectra of aqueous stembark extract of *S. crenata* and its synthesized gold nanoparticles

Table 1: FTIR spectra showing peaks of AuNPs synthesized from aqueous *S. crenata* stem bark extract

Sl. No.	Wave numbers (cm^{-1})	Functional Groups	Bond nature	Compounds
1	2560	S-H stretching	Weak	Thiol
2	2500	O-H stretching	Strong, Broad	Carboxylic Acid
3	2325	O=C=O stretching	Strong	Carbon Dioxide
4	2224	C≡N stretching	Weak	Nitrile
5	2184	C=C=O stretching	Weak	Ketene
6	2162	S-C≡N stretching	Strong	Thiocyanate
7	2115	C≡C stretching	Weak	Alkyne
8	2051	N=C=S stretching	Strong	Isothiocyanate
9	1998	C=C=C stretching	Medium	Allene
10	1951	C-H bending	Weak	Aromatic Compound
11	1909	C=C=C stretching	Medium	Allene
12	1635	C=C stretching	Medium	Alkene
13	1338	S=O stretching	Strong	Sulfonamide
14	1173	C-O stretching	Strong	Ester

4.4. Scanning electron microscopy (SEM) morphological characterization of aqueous stembark extract *S. crenata* AuNPs

The SEM micrograph showed that the synthesized aqueous stembark extract *S. crenata* AuNPs were spherical and well dispersed with an average particle size of 46.8-200nm (Figure-4)

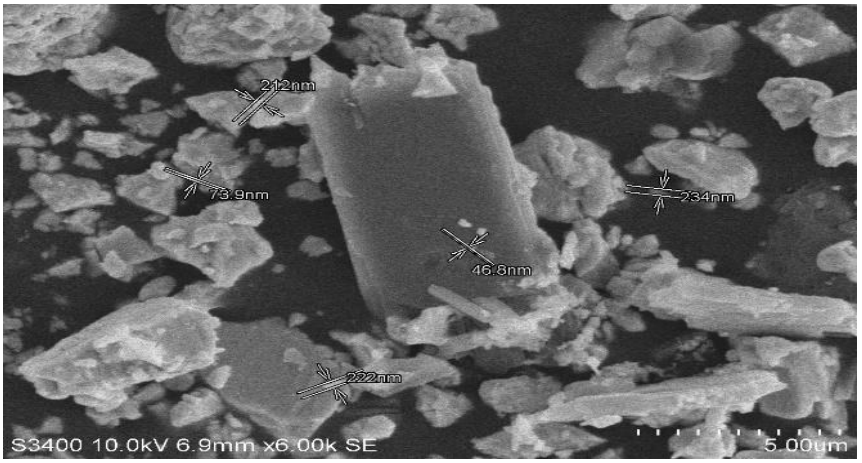

Figure 4: SEM images of AuNPs synthesized from aqueous stem bark extract of *S. crenata*

4.5. XRD analysis of the newly synthesized aqueous *S. crenata* stem bark extract

The crystalline structure of green-synthesized gold nanoparticles (AuNPs) under optimal conditions was confirmed by X-ray diffraction (XRD) analysis (Figure 5). The XRD pattern displayed peaks corresponding to a face-centered cubic (FCC) structure at the following 2θ angles: 9.66°, 14.14°, 22.10°, 28.21°, 31.47°, 32.09°, 37.44°, 38.16°, 40.43°, 44.28°, 49.53°, 50.16°, 58.49°, 64.54°, 73.69°, and 77.53°. These results are consistent with those reported in other studies, which confirm the cubic

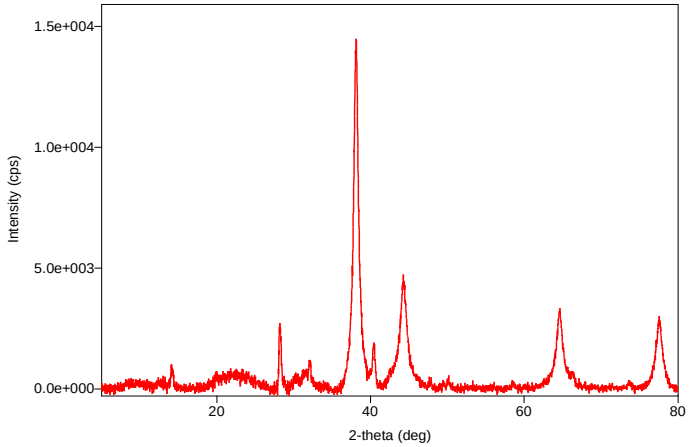

Figure 5: XRD Spectrum of AuNPs synthesized from aqueous stem bark extract of *S. crenata*

4.6. ZETA and PSA analyses of the newly synthesized aqueous *S. crenata* stembark extract

The average hydrodynamic size and dispersion of the gold nanoparticles (AuNPs) were analyzed using a zeta potential analyzer with dynamic light scattering (DLS). DLS analysis indicated that the AuNPs had an average diameter of 71.9 nm (Figure 6A) and zeta potential of -23.5 mV. Additionally, the particle size of the newly synthesized AuNPs was determined to be 93.8 nm (Figure 6B).

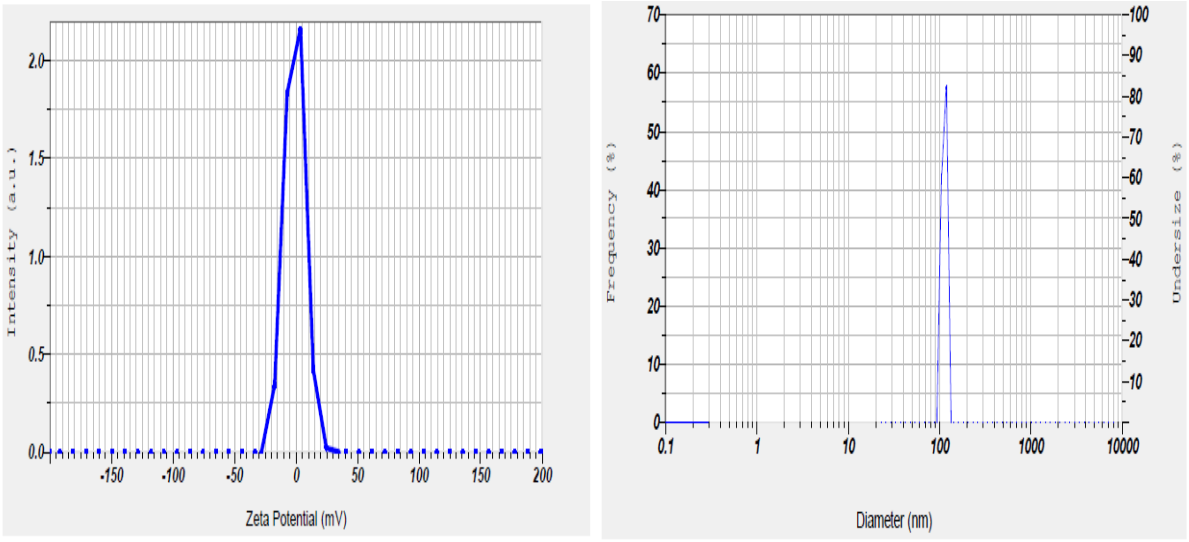

A **B**

Figure-6: A: ZETA potential spectrum of AuNPs synthesized from aqueous stem bark extract of *S. crenata.* **B:** PSA Spectrum of AuNPs synthesized from aqueous stem bark extract of *S. crenata*

4.7. Evaluation of *in vitro* anti-inflammatory activity by the protein denaturation method using newly synthesized aqueous stem bark extract of *S. crenata* AuNPs.

Inflammation is the immune response to specific stimuli, whereas infection involves the invasion of pathogens. Inflammation acts as the body's defense mechanism against injury, illness, or stress and is typically a localized response. Anti-inflammatory medications,

including steroidal and nonsteroidal drugs, are commonly used to manage inflammation, although they can have adverse side effects. Nano-based herbal formulations have been developed to address inflammation, and numerous studies have highlighted the anti-inflammatory properties of metallic nanoparticles derived from plant extracts. In this study, an in vitro protein denaturation assay was performed using aqueous stem bark extracts of *Scolopia crenata* and synthesized gold nanoparticles (AuNPs) to evaluate their anti-inflammatory effects. The anti-inflammatory activity observed in these samples was comparable to that of aspirin, a standard medication. Notable differences in protein denaturation were observed between each group. The results indicated that AuNPs demonstrated significant anti-inflammatory activity, with an inhibition percentage of 80.51±0.02%, closely resembling the 82.36±0.01% inhibition observed with aspirin (Table 2).

Table 2. *In vitro* anti-inflammatory effect of aqueous stem bark extract of *S. crenata* and its synthesized AuNPs nanoparticles

Sl No	Concentration in µg/ml	Std drug Aspirin µg/mL	AuNPs µg/mL
1	**50**	35.84±0.02	36.91±0.04
2	**100**	50.56±0.02	50.78±0.01
3	**150**	61.50±0.01	57.81±0.03
4	**200**	76.02±0.01	73.52±0.02
5	**250**	82.36±0.01	80.51±0.02

Results are expressed as mean ± SD (*n* =3)

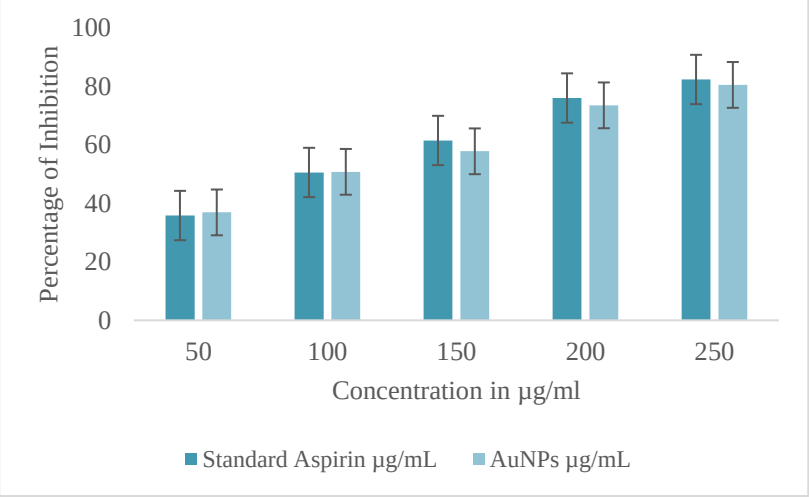

Figure 7. *In vitro* anti-inflammatory effects of the aqueous stem bark extract of *S. crenata* and its synthesized AuNPs.

4.8. Evaluation of *in vitro* wound healing activity by (scratch assay) cell migration assay using newly synthesized aqueous stem bark extract of *S. crenata* AuNPs.

The in vitro wound healing (scratch) assay is a robust method for evaluating cell migration and proliferation under various conditions. In this assay, a wound-like gap was created in a monolayer of proliferating cells using a 200 µL micropipette tip, and the extent of wound closure was measured after applying therapeutic agents and then compared with a control group. In this study, a therapeutic dose of 5 µg/mL, determined via the MTT assay, was used to assess the efficacy of gold nanoparticles (AuNPs) in a wound model generated by the scratch assay in L929 cells (Figure 8A). Treatment with AuNPs synthesized from the aqueous stem

bark extract of *Scolopia crenata* at this concentration resulted in increased wound closure in these cells from 6 to 24 h compared to the control group (Figure 8B). The wound healing potential of AuNPs was confirmed by the scratch assay, which showed 95.42% wound closure compared to 98.76% closure with the standard drug ascorbic acid. This result underscores the wound-healing potential of the formulated AuNPs. This study employed green synthesis of AuNPs using cold maceration of the aqueous extract to evaluate their in vitro wound healing efficiency.

Table 3: *In vitro* scratch assay on normal L929 fibroblast cell line treated with AuNP extract and standard ascorbic acid.

Sl.NO	Samples	Duration in hours	Cell migration in µm	Percentage of wound closure
1	Control	6	4.1	17.30
		12	3.48	
		24	2.1	
2	STD	6	11.98	98.76
		12	7.56	
		24	5.34	
3	AuNPs	6	10.75	95.42
		12	6.36	
		24	3.44	

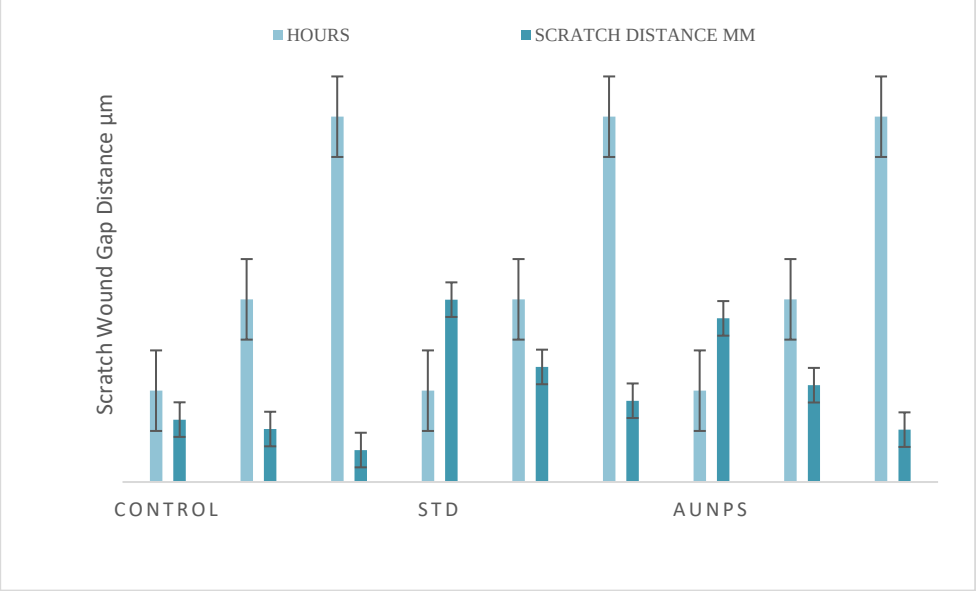

Figure-8: A: Percentage wound closure graph of L929 fibroblasts.

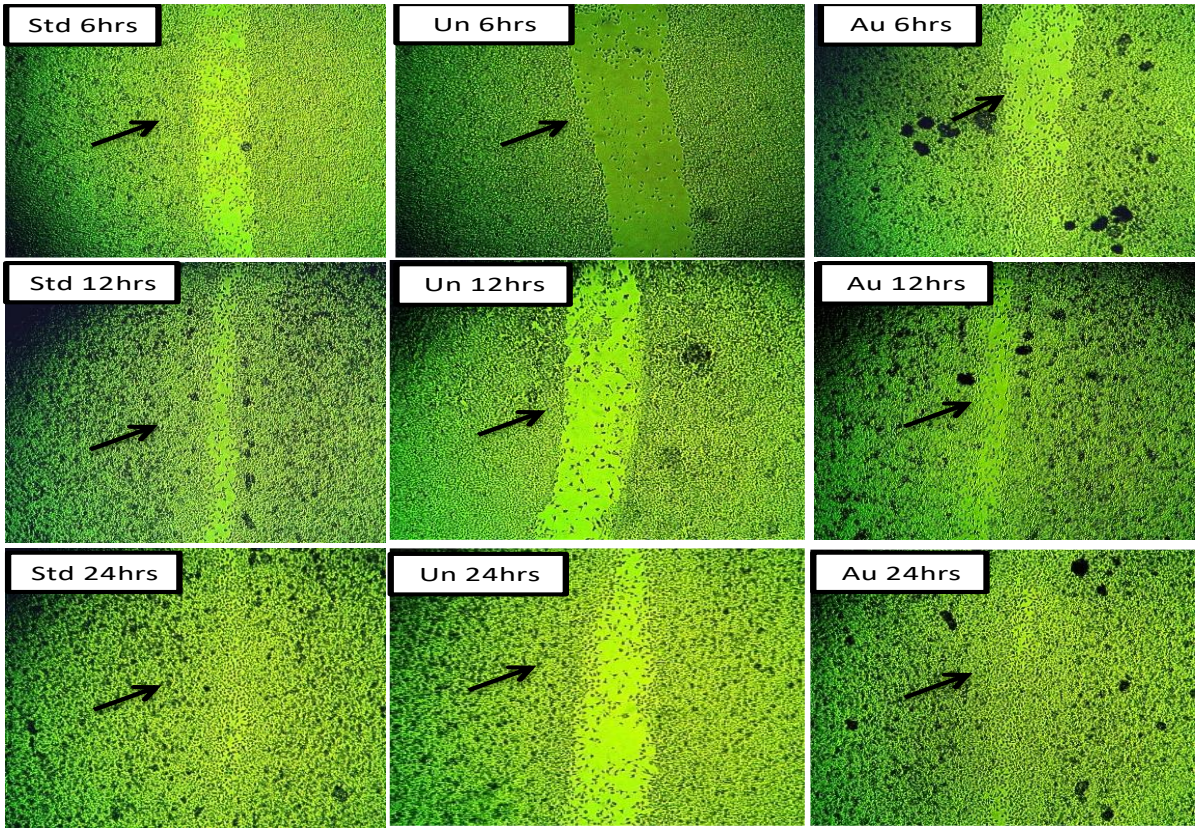

Figure-8: **B:** *In vitro* wound healing assay images of L929 fibroblast cells obtained at 6 to 24 h after wound creation (Au nanoparticles [AuNPs]-5 µg/mL).

4.9. Evaluation of *in vitro* anticancer activity using a newly synthesized aqueous stem bark extract of *S. crenata* AuNPs.

This study investigated the anticancer potential of gold nanoparticles (AuNPs) synthesized from the aqueous stem bark extracts of *S. crenata*. The cytotoxicity and efficacy of these AuNPs were evaluated in noncancerous L929 fibroblast cells and cancerous cell lines, specifically MDA-MB-231 (triple-negative breast cancer) and A549 (lung cancer) (Table 4). The results indicated that AuNPs exhibited significant antiproliferative effects in all tested cell lines (Table 4, Figure 9A). For noncancerous L929 fibroblasts, AuNPs had an IC_{50} value of 78.69 µg/mL, reflecting moderate cytotoxicity (Figure 9B). In contrast, AuNPs demonstrated greater cytotoxicity against cancerous cell lines, with IC_{50} values of 65.05 µg/mL for MDA-MB-231 cells (Figure 9C) and 46.68 µg/mL for A549 cells (Figure 9D). These results suggest that AuNPs are more effective against cancerous cells than against noncancerous cells, highlighting their selective anticancer properties. Although AuNPs are less potent than the standard chemotherapeutic agent cisplatin, which has an IC_{50} range of 1-10 µg/mL for various cancer cell lines, their selective targeting of cancer cells makes them promising candidates for further development in cancer therapy.

Table 4. Percentage of cell viability of gold nanoparticles, L929, MDAMB-231, and A549 cell lines.

Sample	Concentration in µg	Percentage of Cell Viability µg/mL	IC_{50} in µg/mL
L929 cell line	20	87.95±0.01	IC_{50} =78.69 µg/ml
	40	76.22±0.01	
	60	62.68±0.01	
	80	50.10±0.02	
	100	34.86±0.01	
MDAMB-231 cell line	20	84.08±0.01	IC_{50}=65.05 µg/ml
	40	68.86±0.02	
	60	52.81±0.01	
	80	37.17±0.01	
	100	25.78±0.01	
A549 cell line	20	66.50±0.01	IC_{50} =46.68 µg/ml
	40	51.81±0.01	
	60	43.39±0.02	
	80	30.69±0.01	
	100	18.81±0.01	

Results are expressed as mean ± SD (*n* =3)

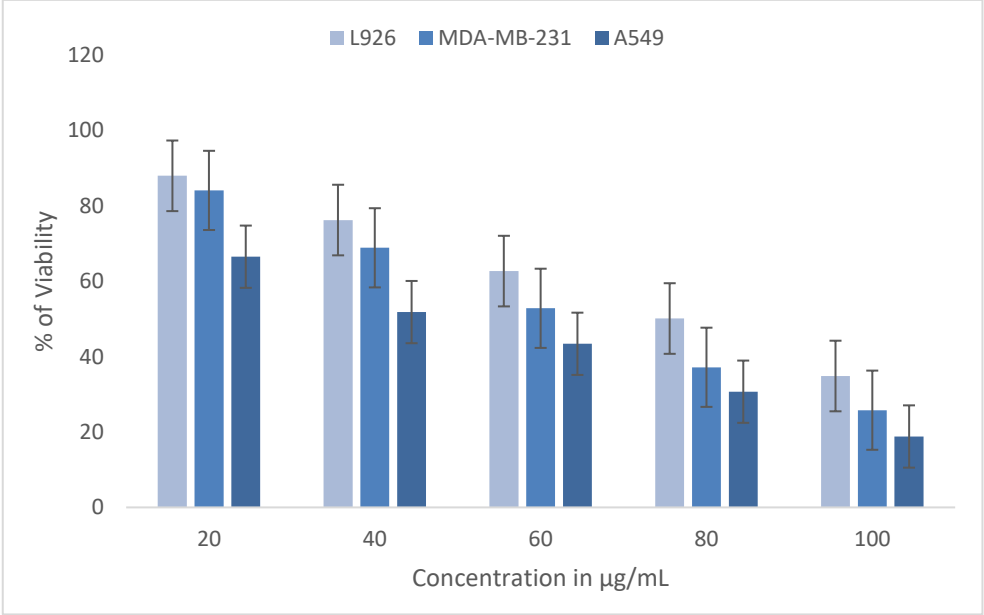

Figure-9: A: Cell viability of L929, MDAMB-231, and A549 cell lines treated with gold nanoparticles.

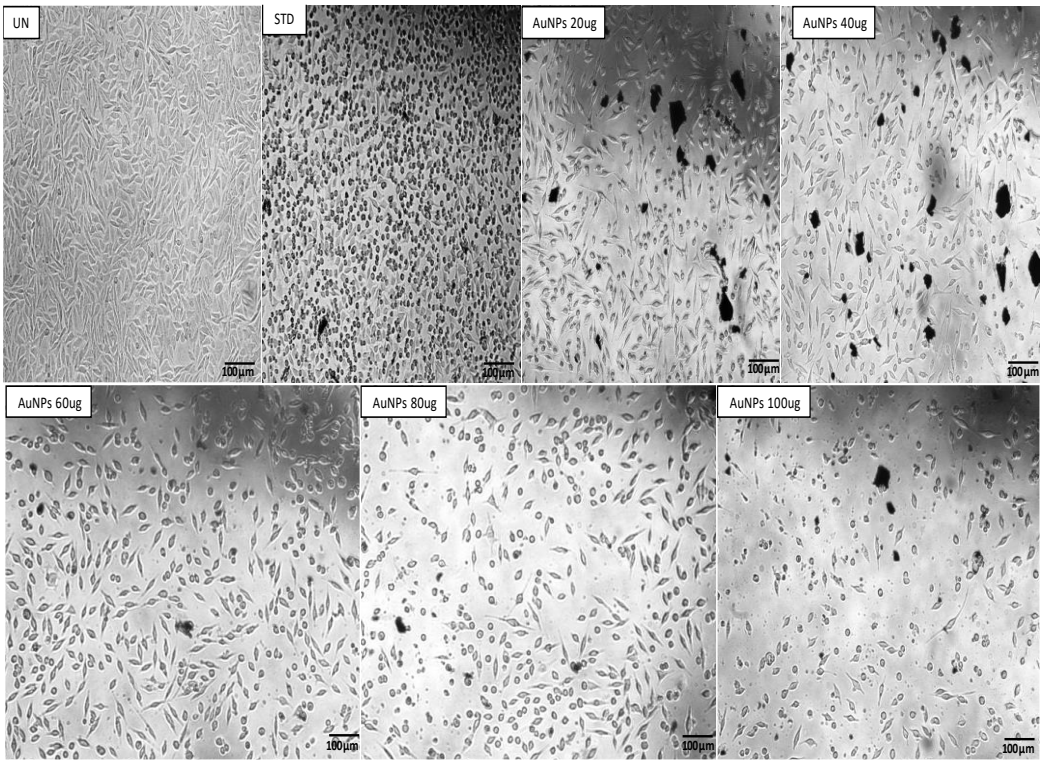

Figure 9: B: Morphological study of the effect of aqueous stem bark extract of *S. crenata* synthesized AuNPs on the L929 cell line.

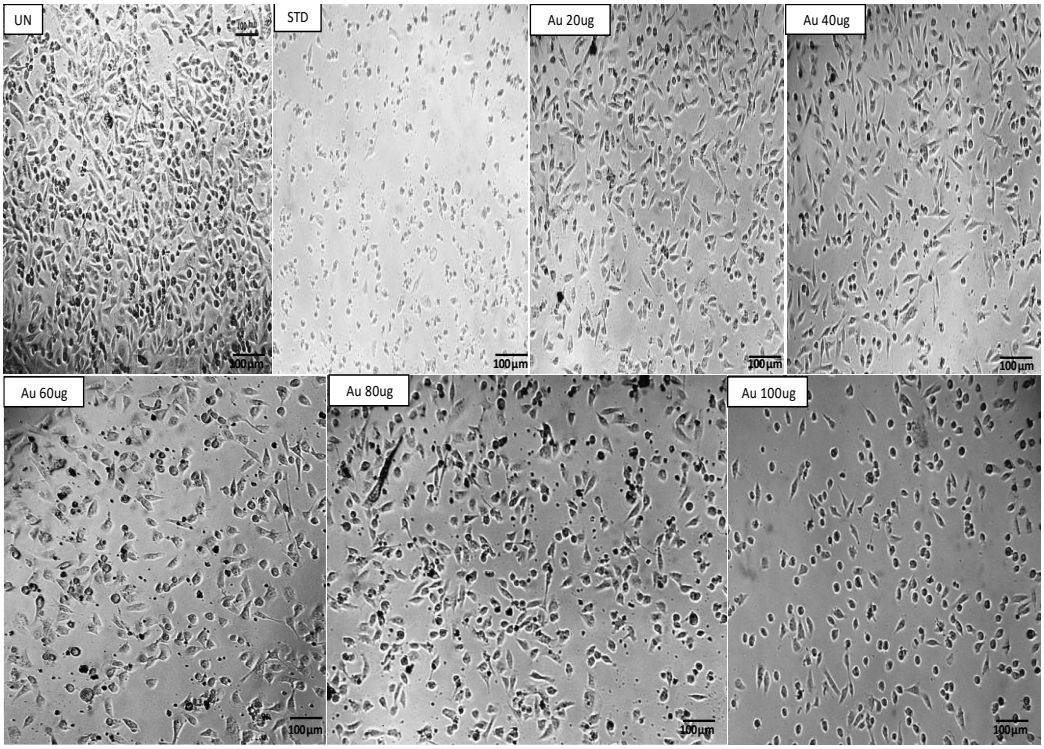

Figure 9: C: Morphological study of the effect of aqueous stem bark extract of *S. crenata* synthesized gold nanoparticles on the MDAMB-231 cell line.

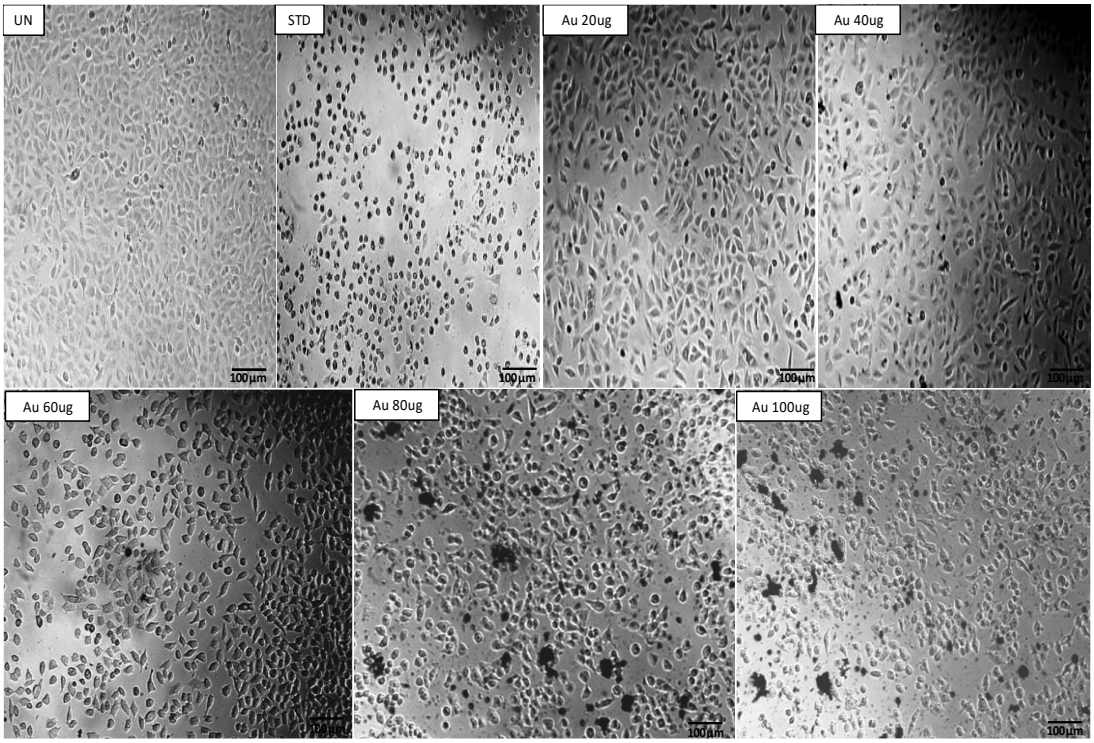

Figure 9: D: Morphological study of the effect of aqueous stem bark extract of *S. crenata* synthesized AuNPs in the A549 cell line.

5. DISCUSSION

This study explored the synthesis and biological activities of gold nanoparticles (AuNPs) using an environmentally friendly method that involves the aqueous stem bark extract of *Scolopia crenata*. The synthesis process was confirmed by a visible color change from brown to dark red after 2 h of incubation, indicating the reduction of Au^+ ions to metallic Au^0 [29]. This reduction is likely facilitated by unidentified biomolecules present in the *S. crenata* extract. The formation of AuNPs was further validated by UV-visible spectroscopy, which revealed a prominent surface plasmon resonance peak at 550 nm, a characteristic feature of AuNPs. Fourier transform infrared spectroscopy (FTIR) was used to identify the functional groups associated with AuNPs. The FTIR spectrum revealed a diverse range of functional groups including alkanes, nitro compounds, alkyl groups, esters, carboxylic acids, alkynes, sulfonamides, allenes, isothiocyanates, ketones, thiocyanate, ketene, nitriles, carbon dioxide, and additional carboxylic acids. These findings suggest that various organic components in plant extracts contribute to the stabilization and reduction of gold ions. The crystalline structure of the synthesized AuNPs was characterized by X-ray diffraction (XRD) analysis, which confirmed their crystalline nature, with a face-centered cubic (FCC) structure typical of gold. The average hydrodynamic size and dispersion of AuNPs were assessed using a zeta potential analyzer coupled with dynamic light scattering (DLS). DLS analysis revealed that the AuNPs had an average diameter of 71.9 nm (Figure 6A) and a zeta potential of -23.5 Â mV, whereas the particle size of the newly synthesized AuNPs was found to be 71.9 nm. The anti-inflammatory potential of AuNPs was evaluated using an in vitro protein denaturation assay by comparing their effects with those of aqueous stem bark extract and standard doses of aspirin[30]. The AuNPs demonstrated significant anti-inflammatory activity, with an inhibition percentage of 80.51±0.02%, which is comparable to the 82.36±0.01% inhibition observed with

aspirin. Additionally, the wound healing efficacy of AuNPs was assessed using an in vitro scratch assay with L929 fibroblast cells[31, 32]. At a concentration of 5 μg/mL, AuNPs facilitated wound closure, resulting in a notable increase in cell migration and a closure percentage of 95.42%. This is nearly equivalent to the closure rate achieved with ascorbic acid, a standard wound healing agent, which recorded a 98.76% closure rate. The anticancer activity of AuNPs has been investigated in noncancerous L929 fibroblast cells and cancerous cell lines, including MDA-MB-231 (triple-negative breast cancer) and A549 (lung cancer)[33, 34]. AuNPs exhibited significant antiproliferative effects, with IC_{50} values of 78.69 μg/mL for L929 cells, 65.05 μg/mL for MDA-MB-231 cells, and 46.68 μg/mL for A549 cells. These results suggest that AuNPs possess selective anticancer properties, showing greater efficacy against cancerous cells than noncancerous cells. While AuNPs are less potent than cisplatin, which has an established IC_{50} range of 15-20 μg/mL for various cancer cell lines, their selective targeting of cancer cells highlights their potential as promising candidates for further research in cancer therapy.

6. CONCLUSION

The results presented here reveal the wound healing and anticancer activities of AuNPs synthesized using the aqueous stem bark extract of *Scolopia crenata*. These findings suggest that the pharmacological properties of *S. crenata* contribute to its anti-inflammatory, wound-healing, and anticancer effects of the gold nanoparticles. Notably, the functionalization of these AuNPs for anticancer applications was achieved without the need for molecular doping, highlighting their potential as effective and fundamentally functional nanomaterials.

Conflicts of interest: The authors declare no conflicts of interest.

Author Contributions: RCK and MGT designed the study and MGT performed the experiments. RCK and MGT analyzed the data from RCK GTM and SAS Composing Surveying and Altering. RCK, MGT, SAS, AS and PM interpreted data and wrote the manuscript. All authors have read and agreed to the published version of the manuscript.

Funding: Not applicable

Data Availability: Not applicable.

REFERENCE

1. Han, G., Ghosh, P., & Rotello, V. M. (2007, February). Functionalized gold nanoparticles for drug delivery. *Nanomedicine*. https://doi.org/10.2217/17435889.2.1.113
2. Sathiyaraj, S., Suriyakala, G., Dhanesh Gandhi, A., Babujanarthanam, R., Almaary, K. S., Chen, T. W., & Kaviyarasu, K. (2021). Biosynthesis, characterization, and antibacterial activity of gold nanoparticles. *Journal of Infection and Public Health*, *14*(12), 1842–1847. https://doi.org/10.1016/j.jiph.2021.10.007
3. Fan, J., Cheng, Y., & Sun, M. (2020, December 1). Functionalized Gold Nanoparticles: Synthesis, Properties and Biomedical Applications. *Chemical Record*. John Wiley and Sons Inc. https://doi.org/10.1002/tcr.202000087
4. Ko, W. C., Wang, S. J., Hsiao, C. Y., Hung, C. T., Hsu, Y. J., Chang, D. C., & Hung, C. F. (2022, March 1). Pharmacological Role of Functionalized Gold Nanoparticles in Disease Applications. *Molecules*. MDPI. https://doi.org/10.3390/molecules27051551

5. Singh, P., Pandit, S., Mokkapati, V. R. S. S., Garg, A., Ravikumar, V., & Mijakovic, I. (2018, July 6). Gold nanoparticles in diagnostics and therapeutics for human cancer. *International Journal of Molecular Sciences*. MDPI AG. https://doi.org/10.3390/ijms19071979
6. Golchin, K., Golchin, J., Ghaderi, S., Alidadiani, N., Eslamkhah, S., Eslamkhah, M., Akbarzadeh, A. (2018, February 17). Gold nanoparticles applications: from artificial enzyme till drug delivery. *Artificial Cells, Nanomedicine and Biotechnology*. Taylor and Francis Ltd. https://doi.org/10.1080/21691401.2017.1305393
7. Mandhata, C. P., Sahoo, C. R., & Padhy, R. N. (2022, December 1). Biomedical Applications of Biosynthesized Gold Nanoparticles from Cyanobacteria: an Overview. *Biological Trace Element Research*. Springer. https://doi.org/10.1007/s12011-021-03078-2
8. Boisselier, E., & Astruc, D. (2009). Gold nanoparticles in nanomedicine: preparations, imaging, diagnostics, therapies and toxicity. *Chemical Society Reviews*, *38*(6), 1759–1782. https://doi.org/10.1039/b806051g
9. Gomathi, R., & Manian, S. (2015). Analgesic and acetylcholinesterase inhibition potential of polyphenols from Scolopia crenata (Flacourtiaceae): An endemic medicinal plant of India. *Industrial Crops and Products*, *73*, 134–143. https://doi.org/10.1016/j.indcrop.2015.03.090
10. Saqr, A. Al, Khafagy, E. S., Alalaiwe, A., Aldawsari, M. F., Alshahrani, S. M., Anwer, M. K., … Hegazy, W. A. H. (2021). Synthesis of gold nanoparticles by using green machinery: Characterization and in vitro toxicity. *Nanomaterials*, *11*(3), 1–14. https://doi.org/10.3390/nano11030808
11. Prasathkumar, M., Anisha, S., Khusro, A., Mohamed Essa, M., Babu Chidambaram, S., Walid Qoronfleh, M., … Emran, T. Bin. (2022). Anti-pathogenic, anti-diabetic, anti-inflammatory, antioxidant, and wound healing efficacy of Datura metel L. leaves. *Arabian Journal of Chemistry*, *15*(9). https://doi.org/10.1016/j.arabjc.2022.104112
12. Tavanappanavar, A. N., Mulla, S. I., Shekhar Seth, C., Bagewadi, Z. K., Rahamathulla, M., Muqtader Ahmed, M., & Ayesha Farhana, S. (2024). Phytochemical analysis, GC–MS profile and determination of antibacterial, antifungal, anti-inflammatory, antioxidant activities of peel and seeds extracts (chloroform and ethyl acetate) of Tamarindus indica L. *Saudi Journal of Biological Sciences*, *31*(1). https://doi.org/10.1016/j.sjbs.2023.103878
13. Li, Z., Zhang, S., Zuber, F., Altenried, S., Jaklenec, A., Langer, R., & Ren, Q. (2023). Topical application of Lactobacilli successfully eradicates Pseudomonas aeruginosa biofilms and promotes wound healing in chronic wounds. *Microbes and Infection*, *25*(8). https://doi.org/10.1016/j.micinf.2023.105176
14. Shabestani Monfared, G., Ertl, P., & Rothbauer, M. (2020). An on-chip wound healing assay fabricated by xurography for evaluation of dermal fibroblast cell migration and wound closure. *Scientific Reports*, *10*(1). https://doi.org/10.1038/s41598-020-73055-7
15. Strachowska, M., Gronkowska, K., Sobczak, M., Grodzicka, M., Michlewska, S., Kołacz, K., … Robaszkiewicz, A. (2023). I-CBP112 declines overexpression of ATP-binding cassette transporters and sensitized drug-resistant MDA-MB-231 and A549 cell lines to chemotherapy drugs. *Biomedicine and Pharmacotherapy*, *168*. https://doi.org/10.1016/j.biopha.2023.115798
16. Rao, P. C., Begum, S., Jahromi, M. A. F., Jahromi, Z. H., Sriram, S., & Sahai, M. (2016). Cytotoxicity of withasteroids: withametelin induces cell cycle arrest at G2/M phase and mitochondria-mediated apoptosis in non-small cell lung cancer A549 cells. *Tumor*

Biology, *37*(9), 12579–12587. https://doi.org/10.1007/s13277-016-5128-5

17. Majdalawieh, A., Kanan, M. C., El-Kadri, O., & Kanan, S. M. (2014). Recent advances in gold and silver nanoparticles: Synthesis and applications. *Journal of Nanoscience and Nanotechnology*. American Scientific Publishers. https://doi.org/10.1166/jnn.2014.9526
18. Santra, T. S., Tseng, F.-G. (Kevin), & Barik, T. K. (2015). Biosynthesis of Silver and Gold Nanoparticles for Potential Biomedical Applications—A Brief Review. *Journal of Nanopharmaceutics and Drug Delivery*, *2*(4), 249–265. https://doi.org/10.1166/jnd.2014.1065
19. Khandanlou, R., Murthy, V., & Wang, H. (2020). Gold nanoparticle-assisted enhancement in bioactive properties of Australian native plant extracts, Tasmannia lanceolata and Backhousia citriodora. *Materials Science and Engineering C*, *112*. https://doi.org/10.1016/j.msec.2020.110922
20. Pal, G., Rai, P., & Pandey, A. (2018). Green synthesis of nanoparticles: A greener approach for a cleaner future. In *Green Synthesis, Characterization and Applications of Nanoparticles* (pp. 1–26). Elsevier. https://doi.org/10.1016/B978-0-08-102579-6.00001-0
21. Mathur, P., Jha, S., Ramteke, S., & Jain, N. K. (2018, October 31). Pharmaceutical aspects of silver nanoparticles. *Artificial Cells, Nanomedicine and Biotechnology*. Taylor and Francis Ltd. https://doi.org/10.1080/21691401.2017.1414825
22. Hosny, M., Fawzy, M., El-Badry, Y. A., Hussein, E. E., & Eltaweil, A. S. (2022). Plant-assisted synthesis of gold nanoparticles for photocatalytic, anticancer, and antioxidant applications. *Journal of Saudi Chemical Society*, *26*(2). https://doi.org/10.1016/j.jscs.2022.101419
23. Gudikandula, K., & Charya Maringanti, S. (2016). Synthesis of silver nanoparticles by chemical and biological methods and their antimicrobial properties. *Journal of Experimental Nanoscience*, *11*(9), 714–721. https://doi.org/10.1080/17458080.2016.1139196
24. Alshehri, A., Ahmad, A., Tiwari, R. K., Ahmad, I., Alkhathami, A. G., Alshahrani, M. Y., … Ansari, I. A. (2022). In Vitro Evaluation of Antioxidant, Anticancer, and Anti-Inflammatory Activities of Ethanolic Leaf Extract of Adenium obesum. *Frontiers in Pharmacology*, *13*. https://doi.org/10.3389/fphar.2022.847534
25. Villegas, L. F., Fernfindez, I. D., Maldonado, H., Torres, R., Zavaleta, A., Vaisberg, A. J., & Hammond, G. B. (1997). *Evaluation of the wound-healing activity of selected traditional medicinal plants from Peril*. *~ Journal of ETHNO-PHARMACOLOGY ELSEVIER Journal of Ethnopharmacology* (Vol. 55).
26. Nguyen, M. H., Lee, S. E., Tran, T. T., Bui, C. B., Nguyen, T. H. N., Vu, N. B. D., … Hadinoto, K. (2019). A simple strategy to enhance the in vivo wound-healing activity of curcumin in the form of self-assembled nanoparticle complex of curcumin and oligochitosan. *Materials Science and Engineering C*, *98*, 54–64. https://doi.org/10.1016/j.msec.2018.12.091
27. Sultana, S., Makeen, H. A., Alhazmi, H. A., Mohan, S., Al Bratty, M., Najmi, A., … Moni, S. S. (2023). Bioactive principles, antibacterial and anticancer properties of Artemisia arborescens L. *Notulae Botanicae Horti Agrobotanici Cluj-Napoca*, *51*(1). https://doi.org/10.15835/nbha51113008
28. Kanjikar, A. P., Hugar, A. L., & Londonkar, R. L. (2018). Characterization of phyto-nanoparticles from Ficus krishnae for their antibacterial and anticancer activities. *Drug Development and Industrial Pharmacy*, *44*(3), 377–384.

https://doi.org/10.1080/03639045.2017.1386205

29. Masse, F., Desjardins, P., Ouellette, M., Couture, C., Omar, M. M., Pernet, V., … Boisselier, E. (2019). Synthesis of ultrastable gold nanoparticles as a new drug delivery system. *Molecules*, *24*(16). https://doi.org/10.3390/molecules24162929
30. Negm, W. A., Elekhnawy, E., Mokhtar, F. A., Binsuwaidan, R., Attallah, N. G. M., Mostafa, S. A., … Eliwa, D. (2024). Phytochemical inspection and anti-inflammatory potential of Euphorbia milii Des Moul. integrated with network pharmacology approach. *Arabian Journal of Chemistry*, *17*(2). https://doi.org/10.1016/j.arabjc.2023.105568
31. Yang, X., Mo, W., Shi, Y., Fang, X., Xu, Y., He, X., & Xu, Y. (2023). Fumaria officinalis-loaded chitosan nanoparticles dispersed in an alginate hydrogel promote diabetic wounds healing by upregulating VEGF, TGF-β, and b-FGF genes: A preclinical investigation. *Heliyon*, *9*(7). https://doi.org/10.1016/j.heliyon.2023.e17704
32. Kokane, D. D., More, R. Y., Kale, M. B., Nehete, M. N., Mehendale, P. C., & Gadgoli, C. H. (2009). Evaluation of wound healing activity of root of Mimosa pudica. *Journal of Ethnopharmacology*, *124*(2), 311–315. https://doi.org/10.1016/j.jep.2009.04.038
33. Pandey, B. P., Adhikari, K., Pradhan, S. P., Shin, H. J., Lee, E. K., & Jung, H. J. (2020). In-vitro antioxidant, anti-cancer, and anti-inflammatory activities of selected medicinal plants from western Nepal. *Future Journal of Pharmaceutical Sciences*, *6*(1). https://doi.org/10.1186/s43094-020-00107-0
34. Sajid, M., Yan, C., Li, D., Merugu, S. B., Negi, H., & Khan, M. R. (2019). Potent anti-cancer activity of Alnus nitida against lung cancer cells; in vitro and in vivo studies. *Biomedicine and Pharmacotherapy*, *110*, 254–264. https://doi.org/10.1016/j.biopha.2018.11.138